https://doi.org/10.15407/ujpe65.10.898

D.M. POLISHCHUK,[1,2] M.M. KULYK,[1,3] E. HOLMGREN,[1] G. PASQUALE,[1] A.F. KRAVETS,[2] V. KORENIVSKI[1]

[1] Nanostructure Physics, Royal Institute of Technology
(Roslagstullsbacken 21, Stockholm 11421, Sweden; e-mail: dpol@kth.se)
[2] Institute of Magnetism, Nat. Acad. of Sci. of Ukraine
and Ministry of Education and Science of Ukraine
(36b, Academician Vernadsky Blvd., Kyiv 03142, Ukraine)
[3] Institute of Physics, Nat. Acad. of Sci. of Ukraine
(46, Nauky Ave., Kyiv 03028, Ukraine)

INFLUENCE OF NANOSIZE EFFECT AND NON-MAGNETIC DILUTION ON INTERLAYER EXCHANGE COUPLING IN Fe–Cr/Cr NANOSTRUCTURES

Magnetic properties of multilayered [Fe–Cr/Cr]× 8 nanostructures with the interlayer exchange coupling of the antiferromagnetic type and without the interlayer coupling have been studied. The values of the saturation magnetization and the interlayer exchange coupling constant are shown to strongly depend on the thickness and non-magnetic dilution of the Fe–Cr layers. It is found that those parameters differently affect the interlayer exchange coupling, which is explained by an interplay between the size effect (the thickness of the Fe–Cr layers) and the magnetic polarization of the Fe–Cr/Cr interfaces depending on the Fe concentration.

K e y w o r d s: ferromagnetic film, multilayered nanostructure, size effect, interlayer exchange coupling, dilute ferromagnetic alloy.

1. Introduction

The discoveries of the indirect oscillating interlayer exchange coupling [1] and the giant magnetoresistance effect [2, 3] in multilayered magnetic nanostructures with alternating layers of ferromagnets (FM) and non-magnetic metals (NM) gave impetus to the emergence of the spintronics industry [4–6]. Owing to its exchange origin [7, 8], the indirect coupling is characterized by a much larger strength in comparison with other types of interlayer coupling, e.g., the magnetostatic Néel interaction [9, 10]. Furthermore, by choosing the NM layer thickness, both the coupling strength and the coupling type (the ferromagnetic or antiferromagnetic ordering of the magnetic moments of the FM layers) can be controlled [11, 12]. Such properties are attractive for the development of various magnetic functional materials [13–15]. In particular, the antiferromagnetic coupling between the layers forms a basis for the production of synthetic antiferromagnets, which are used in magnetic sensors [16,17] and as elements of magnetic random access memory (MRAM) [18–20], being also promising systems for antiferromagnetic spintronics [21], which is being actively developed now [22, 23].

The indirect interlayer exchange coupling can lead to interesting interesting thermomagnetic phenomena in multilayered FM/NM systems near the Curie temperature for the FM layers [24–29]. For instance, such phenomena as the temperature-induced switching of the interlayer coupling from the ferromagnetic to antiferromagnetic type [17, 28] and the giant magnetocaloric effect [29] have been demonstrated recently for systems based on multilayered Fe–Cr/Cr nanostructures (Fig. 1, *a*), where Fe–Cr are layers of dilute ferromagnetic alloys Fe_xCr_{100-x} with the Curie temperature close to room temperature (Fig. 1, *b*). Those phenomena were explained as a result of the competition between the internal exchange coupling inside the layers of dilute Fe–Cr ferromagnets and the interlayer exchange coupling that acts on the Fe–Cr

layers from outside. Since the interlayer coupling is an interfacial effect, the revealed phenomena were found to be the most pronounced for thin Fe–Cr layers about 1 nm in thickness. For thicknesses close to this value, other nanoscale effects emerging owing to an increase in the ratio between the number of spins at the interface and in the bulk of the FM layers can also make a significant contribution, which has not been discussed in detail in the above-cited works.

This work aims at at a systematic research of the interlayer exchange coupling in antiferromagnetically coupled Fe-Cr/Cr multilayers, as well as its dependence on the thickness of Fe–Cr layers and their dilution with non-magnetic Cr atoms. Using magnetometric measurements, the values of the saturation magnetization and the interlayer coupling constant were obtained for various thicknesses of the Fe–Cr layers and Fe concentrations in them, which allowed us to characterize the influence of size effects and the non-magnetic dilution on the magnetostatic behavior of the examined system.

2. Samples and Experiment Details

Multilayers $[Fe_xCr_{100-x}(d)/Cr(d_{Cr})] \times 8$ (with $d = 2$, 3, and 5 nm; $x = = 37$, 45, 50, and 55 at% Fe; and $d_{Cr} = 1.2$ and 3.0 nm) were deposited at room temperature onto single-crystalline Si(100) substrates using magnetron sputtering. The deposition was performed on an ultrahigh-vacuum ATC Orion AJA International setup with the base pressure $p_b \sim$ $\sim 10^{-8}$ Torr. A thin naturally formed amorphous layer of silicon oxide was removed from the substrate surface by Ar plasma etching right before deposition. As a result, the antiferromagnetic interlayer exchange in the Fe–Cr/Cr structures became substantially stronger.

The thicknesses of the magnetic Fe–Cr layers and non-magnetic Cr ones were controlled by selecting their deposition times at the given deposition rates. The latter were determined after their calibration using nanoprofilometry. The layers of dilute ferromagnetic alloys Fe_xCr_{100-x} were deposited using co-sputtering from separate Fe and Cr targets, respectively. The composition of Fe_xCr_{100-x} alloys was controlled by selecting the corresponding deposition rates for the individual components. Since the surface roughness increases with the number of bilayers, N,

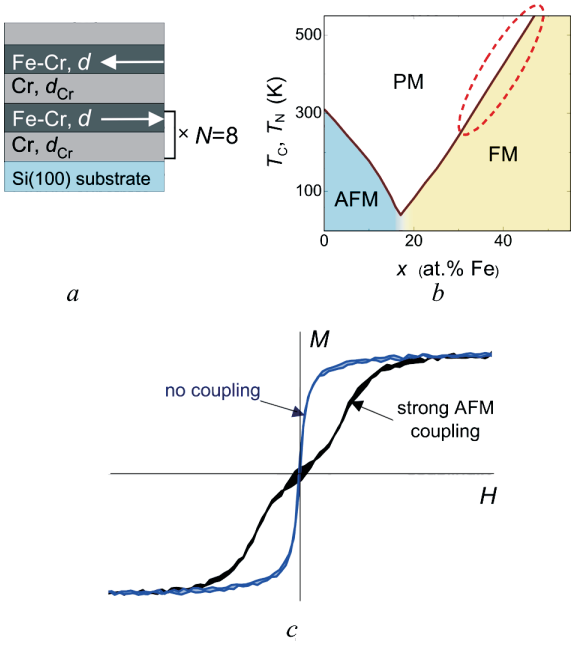

Fig. 1. Schematic representation of the studied multilayered nanostructures (a), phase diagram of the dilute ferromagnetic alloy Fe_xCr_{100-x} [27] (b), and typical magnetization curves $M(H)$ for the Fe–Cr/Cr structures with and without the antiferromagnetic interlayer coupling (c)

and affects the interlayer coupling between the upper layers, the optimal number $N = 8$ was determined, for which the corresponding effects were negligibly small.

In this work, two sample series were studied. In the first series, the concentration of Fe atoms in the Fe–Cr layers was constant ($x = 37$ at% Fe), whereas the layer thickness was varied ($d = 2$, 3, and 5 nm). Below, the structures belonging to this series will be referred to as $Fe_{37}Cr_{63}(d)/Cr(d_{Cr})$. In the second series, the thickness of the Fe–Cr layers was constant ($d = 1.2$ nm), but the Fe concentration in them was varied ($x = 37$, 45, 50, and 55 at% Fe). The structures of this series will be referred to as $Fe_xCr_{100-x}(1.2\text{ nm})/Cr(d_{Cr})$. The both series consisted of samples of two types, which were different in the thickness of their Cr layers ($d_{Cr} = 1.2$ and 3.0 nm). The thickness $d_{Cr} = 1.2$ nm corresponded to the maximum of the antiferromagnetic exchange coupling between the Fe–Cr layers (see the corresponding curve in Fig. 1, c), which was found while analyzing an additional series of the Fe–Cr/Cr structures with different thicknesses of the Cr layer, d_{Cr}. In par-

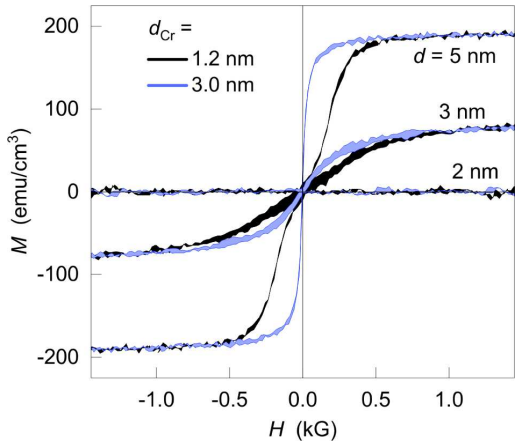

Fig. 2. Magnetization curves $M(H)$ for the $Fe_{37}Cr_{63}(d)$/$Cr(d_{Cr} = 1.2$ and 3.0 nm) structures with various thicknesses of the dilute Fe–Cr layers $d = 2$, 3, and 5 nm

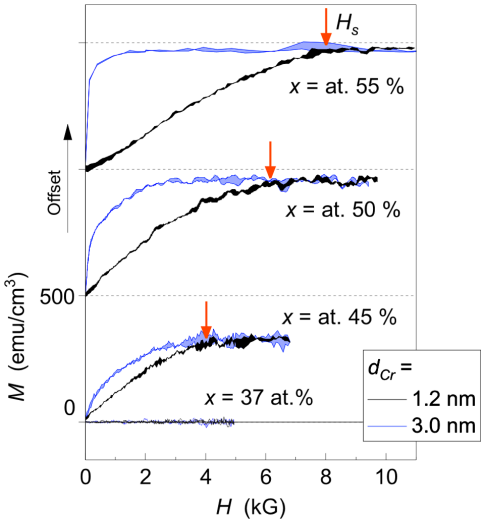

Fig. 3. Magnetization curves $M(H)$ for the Fe_xCr_{100-x}(1.2 nm)/$Cr(d_{Cr} = 1.2$ and 3.0 nm) structures with various Fe concentrations in the dilute Fe-Cr layers $x = 37$, 45, 50, and 55 at% Fe. To make the comparison more convenient, the $M(H)$ curves for different concentrations are shifted with respect to one another along the M-axis

ticular, the absence of exchange interaction in the Fe–Cr/Cr structures with $d_{Cr} \geq 3$ nm was revealed (Fig. 1, *c*).

The magnetic properties of multilayered nanostructures were studied using vibration magnetometry (Lakeshore Inc.) at room temperature. The magnetic field was applied in the film plane. The ferromagnetic contribution to the total magnetic signal from the structures was calculated by subtracting the background signal that was measured for pure silicon substrates with the same volume as for the samples in the main series. The obtained data were normalized by the volume of the Fe_xCr_{100-x} layers. The latter was calculated on the basis of the nominal layer thickness and the measured sample area.

3. Experimental Results

Figure 2 exhibits the magnetization curves $M(H)$ measured for the $Fe_{37}Cr_{63}(d)/Cr(d_{Cr})$ structures with various thicknesses of both the dilute Fe–Cr layers ($d = 2$, 3, and 5 nm) and the Cr layers ($d_{Cr} =$ $= 1.2$ and 3.0 nm). The curves $M(H)$ demonstrate a pronounced dependence on both d and d_{Cr}. The $M(H)$ curve for the $Fe_{37}Cr_{63}$(5 nm)/Cr(3 nm) structure has characteristic features inherent to a thin ferromagnetic film near the Curie point. An almost zero value of the coercive field together with a gradual tendency to the saturation indicates an influence of temperature fluctuations on the magnetic ordering in the $Fe_{37}Cr_{63}$(5 nm) layers. At the same time, the $M(H)$ curve for the $Fe_{37}Cr_{63}$(5 nm)/Cr(1.2 nm) structure with thin Cr layers reveals rather strong interlayer exchange coupling between the $Fe_{37}Cr_{63}$(5 nm) layers. The zero value of the residual magnetization, low susceptibility in the zero field, and rather high saturation field ($H_s \approx 500$ G) indicates the antiferromagnetic type of the interlayer coupling. The $M(H)$ curves for $d_{Cr} = 1.2$ and 3.0 nm reach the same saturation magnetization $M_s \approx 190$ emu/cm^3 in the fields $H > H_s \approx 500$ G.

The magnetization curves $M(H)$ considerably change with the decrease of the Fe–Cr layer thickness (Fig. 2). The $M(H)$ loops for the $Fe_{37}Cr_{63}$(3 nm)/Cr structures demonstrate features that are similar to those available in the magnetization curves for the structures with $d = 5$ nm. In particular, these are different saturation fields H_s, which is associated with the presence of the interlayer exchange coupling in the structure with $d_{Cr} = 1.2$ nm and its absence in the structure with $d_{Cr} = 3$ nm. However, the saturation magnetization of the $Fe_{37}Cr_{63}$(3 nm)/Cr structures is substantially lower, $M_s \approx 80$ emu/cm^3, which can be attributed to to a decrease of the effective Curie temperature T_{C*} for the $Fe_{37}Cr_{63}$(3 nm) layers [30]. The $Fe_{37}Cr_{63}$(2 nm)/Cr structures do not reveal any ferromagnetic behavior at all, which can be explained by the reduced T_{C*} in the $Fe_{37}Cr_{63}$(2 nm) layers well below room temperature.

In Fig. 3, the magnetization curves $M(H)$ are depicted for the structures $Fe_xCr_{100-x}(1.2\ nm)/Cr(d_{Cr} = 1.2$ and 3.0 nm) with a fixed thickness of the Fe–Cr ferromagnetic layers ($d = 1.2$ nm) and various Fe concentrations ($x = 37$, 45, 50, and 55 at% Fe). As the Fe concentration increases, the saturation magnetization M_s expectedly grows: from 330 emu/cm^3 at 45 at% Fe to 490 emu/cm^3 at 55 at% Fe. It should be noted that the values obtained for M_s are approximately 40% lower than the corresponding values obtained for bulk samples from magnetometric measurements of thick films (about 30 nm), which is evidently associated with the nanosize effect. Simultaneously with the growth of M_s at higher x-concentrations, the saturation field H_s also increases for the structures with interlayer coupling ($d_{Cr} = 1.2$ nm): from 4.0 kG for 45 at% Fe to 8.1 kG for 55 at% Fe. The specimen with $x = 37$ at% Fe did not reveal the ferromagnetic behavior, because the Curie temperature T_{C*} for its $Fe_{37}Cr_{63}(1.2\ nm)$ layers is low.

In Fig. 4, the dependences of the saturation magnetization M_s and the interlayer coupling constant J_{ex} on the thickness d and the Fe concentration x are shown for the $Fe_xCr_{100-x}(d)/Cr(1.2\ nm)$ structures. The constant J_{ex} was calculated according to the expression $J_{ex} = dM_sH_s$ [31], where H_s is the saturation field. The latter was determined for the considered structures as the field, where the $M(H)$ curves converge at $d_{Cr} = 1.2$ nm (the coupled state) or 3.0 nm (no interlayer coupling) (the corresponding values are indicated by arrows in Fig. 3).

The saturation magnetization M_s of the $Fe_xCr_{100-x}(d)$ layers increases both with the layer thickness d at the constant concentration $x = const = 37$ at% Fe and with the Fe concentration x at the constant layer thickness $d = 1.2$ nm. This behavior is natural. The character of changes in the values of the interlayer coupling constant J_{ex} is a little different for the two series of specimens. For the series of $Fe_{37}Cr_{63}(d)/Cr(d_{Cr})$ structures with various thicknesses d, the growth of J_{ex} linearly correlates with an increase of the saturation magnetization M_s. Namely, the both quantities have a 2.5-fold increase, when the thickness d changes from 3 to 5 nm. But, for the series of $Fe_xCr_{100-x}(1.2\ nm)/Cr$ structures with various Fe concentrations x, the ratio between M_s and J_{ex} changes substantially. In particular, as the concentration x grows by 10%, the value of J_{ex} increases by a factor of 3.5, whereas the value of M_s only by a factor of 1.5.

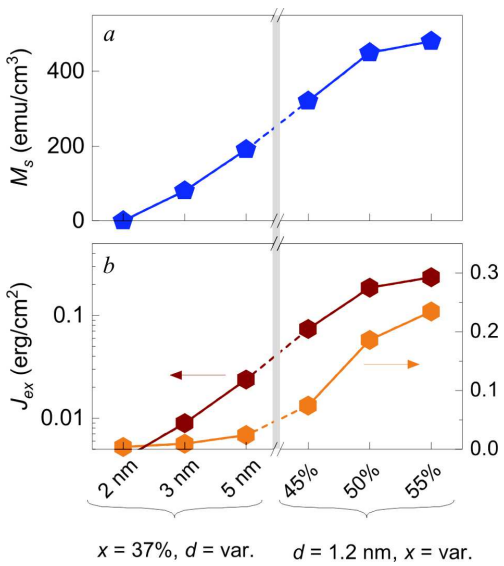

Fig. 4. Dependences of the saturation magnetization M_s (a) and the interlayer coupling constant J_{ex} on the thickness d of the Fe_xCr_{100-x} layers and the Fe concentration x in them (b)

4. Discussion and Conclusions

The increase of the saturation magnetization with the growth of the Fe–Cr layer thickness, which is shown in Figs. 2 and 4, a, should be associated with the nanosize effect [32, 33]. According to the latter, when the thickness of the FM layers decreases, the ratio of surface-to-bulk spins increases – they are more weakly bound by the exchange coupling because of the absence of magnetic neighbors in the non-magnetic layer. Hence, those spins are more sensitive to temperature fluctuations, which manifests itself as a reduction in the effective Curie temperature of the whole FM layer. Thus, the increase of the saturation magnetization with the Fe–Cr layer thickness or with the concentration of Fe atoms in them (Fig. 4, a) is associated with the increase of the effective Curie temperature T_{C*} of the Fe–Cr layers.

The interlayer exchange coupling constant J_{ex} is proportional to the magnetic polarization of atomic spins at the FM/NM interface [8, 34], which, in turn, is usually proportional to the saturation magnetization M_s of the FM layers. This proportionality between J_{ex} and M_s is observed for the Fe–Cr/Cr

structures with the constant Fe concentration $x = 37$ at% but different thicknesses of the Fe–Cr layers (Fig. 4, *b*). However, for the structures with the constant thickness of Fe–Cr layers, $d = 1.2$ nm, but with different Fe concentrations x, the proportionality between J_{ex} and M_s changes. Namely, the concentration growth is more strongly reflected in the increase of the J_{ex} constant than in the increase of the M_s value. From whence, a conclusion can be drawn that the growth in the concentration of magnetic atoms at the interface affects the interlayer coupling more strongly than the growth of the effective magnetization of the FM layers. This conclusion is in agreement with the known literature data concerning the application of Fe or Co monolayers deposited onto a weakly magnetic FM/NM interface in order to enhance the interlayer coupling [35].

Thus, the magnetometric studies of multilayered Fe–Cr/Cr structures made it possible to analyze the influence of the thickness of the ferromagnetic Fe–Cr layers and the Fe concentration in them on the interlayer exchange coupling. The values of the saturation magnetization and the interlayer coupling constant, as well as their dependences on the indicated parameters, were obtained. For the series of structures with different thicknesses of the Fe–Cr layers but a constant Fe concentration in them, the interlayer coupling strength was found to be proportional to the saturation magnetization. A conclusion was made that a decrease in the thickness of the FM layers results in a reduction of the effective Curie temperature because of nanoscale effects. For the series of structures with a constant thickness of the Fe–Cr layers but different Fe concentrations in them, the enhancement of the interlayer exchange coupling turned out much more pronounced than the growth of the saturation magnetization. It was concluded that the growth in the concentration of magnetic Fe atoms at the Fe–Cr/Cr interface effectively strengthens the interlayer coupling by enhancing the magnetic polarization of the interfaces.

The work was partially sponsored by the National Academy of Sciences of Ukraine (projects Nos. 0120U100457 and 0118U003265), as well as by the Swedish Stiftelse Olle Engkvist Byggmästare, the Swedish Institute Visby Program 2019/20, and the Swedish Research Council (VR Grant 2018-03526).

1. P. Grünberg *et al.* Layered magnetic structures: Evidence for antiferromagnetic coupling of Fe layers across Cr interlayers. *J. Appl. Phys.* **61**, 3750 (1986).
2. M.N. Baibich *et al.* Giant magnetoresistance of (001)Fe/(001)Cr magnetic superlattices. *Phys. Rev. Lett.* **61**, 2472 (1988).
3. G. Binasch, P. Grünberg, F. Saurenbach, W. Zinn. Enhanced magnetoresistance in layered magnetic structures with antiferromagnetic interlayer exchange. *Phys. Rev. B* **39**, 4828 (1989).
4. P. Grünberg. Layered magnetic structures: History, highlights, applications. *Phys. Today* **54**, 31 (2001).
5. I. Žutić, J. Fabian, S. Das Sarma. Spintronics: Fundamentals and applications. *Rev. Mod. Phys.* **76**, 323 (2004).
6. J. Sinova, I. Žutić. New moves of the spintronics tango. *Nat. Mater.* **11**, 368 (2012).
7. P. Bruno. Interlayer exchange coupling: A unified physical picture. *J. Magn. Magn. Mater.* **121**, 248 (1993).
8. M.D. Stiles. Exchange coupling in magnetic heterostructures. *Phys. Rev. B* **48**, 7238 (1993).
9. L. Néel. Magnetisme-sur un nouveau mode de couplage entre les animantations de deux couches minces ferromagnetiques. *Compt. Rend.* **255**, 1676 (1962).
10. J.C.S. Kools, W. Kula, D. Mauri, T. Lin. Effect of finite magnetic film thickness on Néel coupling in spin valves. *J. Appl. Phys.* **85**, 4466 (1999).
11. S.S.P. Parkin, N. More, K.P. Roche. Oscillations in exchange coupling and magnetoresistance in metallic superlattice structures: Co/Ru, Co/Cr, and Fe/Cr. *Phys. Rev. Lett.* **64**, 2304 (1990).
12. S.S.P. Parkin, R.Bhadra, K.P. Roche. Oscillatory magnetic exchange coupling through thin copper layers. *Phys. Rev. Lett.* **66**, 2152 (1991).
13. S. Bandiera *et al.* Comparison of synthetic antiferromagnets and hard ferromagnets as reference layer in magnetic tunnel junctions with perpendicular magnetic anisotropy. *IEEE Magn. Lett.* **1**, 3000204 (2010).
14. Y.-C. Lau, D. Betto, K. Rode, J.M.D. Coey, P. Stamenov. Spin–orbit torque switching without an external field using interlayer exchange coupling. *Nat. Nanotechnol.* **11**, 758 (2016).
15. T. Newhouse-Illige *et al.* Voltage-controlled interlayer coupling in perpendicularly magnetized magnetic tunnel junctions. *Nat. Commun.* **8**, 15232 (2017).
16. J.G. Zhu. Spin valve and dual spin valve heads with synthetic antiferromagnets. *IEEE Trans. Magn.* **35**, 655 (1999).
17. S. Parkin *et al.* Magnetically engineered spintronic sensors and memory. *Proc. IEEE* **91**, 661 (2003).
18. J.M. Slaughter *et al.* Fundamentals of MRAM technology. *J. Supercond.* **15**, 19 (2002).
19. A. Bergman *et al.* Ultrafast switching in a synthetic antiferromagnetic magnetic random-access memory device. *Phys. Rev. B* **83**, 224429 (2011).
20. D. Apalkov, B. Dieny, J.M. Slaughter. Magnetoresistive random access memory. *Proc. IEEE* **104**, 1796 (2016).

21. R.A. Duine, K.-J. Lee, S.S.P. Parkin, M.D. Stiles. Synthetic antiferromagnetic spintronics. *Nat. Phys. 14*, 217 (2018).
22. E.V. Gomonay, V.M. Loktev. Spintronics of antiferromagnetic systems (Review Article). *Low Temp. Phys.* **40**, 17 (2014).
23. V. Baltz *et al.* Antiferromagnetic spintronics. *Rev. Mod. Phys.* **90**, 015005 (2018).
24. K.M. Döbrich *et al.* Temperature-induced reversal of magnetic interlayer exchange coupling. *Phys. Rev. Lett.* **100**, 227203 (2008).
25. Z.Y. Liu *et al.* Thermally induced antiferromagnetic interlayer coupling and its oscillatory dependence on repetition number in spin-valve Co/Pt multilayers. *J. Phys. D* **42**, 035010 (2009).
26. T. Mukherjee, S. Sahoo, R. Skomski, D.J. Sellmyer, C. Binek. Magnetocaloric properties of Co/Cr superlattices. *Phys. Rev. B* **79**, 144406 (2009).
27. *Magnetic Properties of Metals.* Edited by H.P.J. Wijn (Springer, 1991).
28. D.M. Polishchuk, Y.O. Tykhonenko-Polishchuk, E. Holmgren, A.F. Kravets, V. Korenivski. Thermally induced antiferromagnetic exchange in magnetic multilayers. *Phys. Rev. B* **96**, 104427 (2017).
29. D.M. Polishchuk *et al.* Giant magnetocaloric effect driven by indirect exchange in magnetic multilayers. *Phys. Rev. Mater.* **2**, 114402 (2018).
30. A.F. Kravets *et al.* Temperature-controlled interlayer exchange coupling in strong/weak ferromagnetic multilayers: A thermomagnetic Curie switch. *Phys. Rev. B* **86**, 1 (2012).
31. Z. Zhang, L. Zhou, P.E. Wigen, K. Ounadjela. Angular dependence of ferromagnetic resonance in exchange-coupled Co/Ru/Co trilayer structures. *Phys. Rev. B* **50**, 6094 (1994).
32. C.M. Schneider *et al.* Curie temperature of ultrathin films of fcc-cobalt epitaxially grown on atomically flat Cu(100) surfaces. *Phys. Rev. Lett.* **6**4, 1059 (1990).
33. F. Huang, M.T. Kief, G.J. Mankey, R.F. Willis. Magnetism in the few-monolayers limit: A surface magneto-optic Kerr-effect study of the magnetic behavior of ultrathin films of Co, Ni, and Co–Ni alloys on Cu(100) and Cu(111). *Phys. Rev. B* **49**, 3962 (1994).
34. P. Bruno. Theory of interlayer magnetic coupling. *Phys. Rev. B* **52**, 411 (1995).
35. S.S. Parkin. Dramatic enhancement of interlayer exchange coupling and giant magnetoresistance in $Ni_{81}Fe_{19}$/Cu multilayers by addition of thin Co interface layers. *Appl. Phys. Lett.* **61**, 1358 (1992).

Received 10.07.20.
Translated from Ukrainian by O.I. Voitenko

Д.М. Поліщук, М.М. Кулик, Е. Холмгрен, Г. Паскуале, А.Ф. Кравець, В. Коренівський

ВПЛИВ НАНОРОЗМІРНОГО ЕФЕКТУ ТА НЕМАГНІТНОГО РОЗБАВЛЕННЯ НА МІЖШАРОВУ ОБМІННУ ВЗАЄМОДІЮ В БАГАТОШАРОВИХ СТРУКТУРАХ Fe–Cr/Cr

Р е з ю м е

Досліджено магнітні властивості обмінно зв'язаних багатошарових наноструктур $[Fe_xCr_{100-x}(d)/Cr(d_{Cr})] \times 8$ (d = 2, 3 і 5 нм; x = 37, 45, 50 і 55 ат.% Fe; d_{Cr} = 1,2 та 3,0 нм). Аналіз проводиться для структур з антиферомагнітним типом міжшарової обмінної взаємодії (d_{Cr} = 1,2 нм) та структур з відсутнім міжшаровим зв'язком (d_{Cr} = 3 нм). Виявлено значні зміни у значеннях намагніченості насичення та константи міжшарової взаємодії в залежності від товщини шарів Fe–Cr та їх немагнітного розбавлення. Встановлено, що ці параметри по-різному впливають на міжшарову обмінну взаємодію. Це пояснюється взаємозв'язком між нанорозмірним ефектом, чутливим до товщини Fe–Cr шарів, та магнітною поляризацією інтерфейсів Fe–Cr/Cr, яка пропорційна концентрації Fe.